Zero-bias conductance vanishing induced by the same-spin-band Andreev reflection in half-metallic ferromagnet/superconductor contacts

C. D. Feng, Zhi Ming Zheng, R. Shen, Baigeng Wang, and D. Y. Xing
National Laboratory of Solid State Microstructures and Department of Physics, Nanjing University, Nanjing 210093, China
(Received 10 May 2010; published 10 June 2010)

The Blonder-Tinkham-Klapwijk approach is extended to study conductance spectra of half-metallic ferromagnet/*s*-wave superconductor contacts. It is found that a distinct Andreev reflection (AR) does exist in which the incident electron and the Andreev-reflected hole belong to the same-spin subband, provided that spin-flip scattering is present at the interface. The predicted distinguishing mark of the same-spin-band AR is the zero-bias conductance vanishing and finite V-shape conductance within the energy gap. Its experimental observation will provide a conclusive proof for the same-spin-band AR and also a best judgement about the half-metallic ferromagnet.

DOI: 10.1103/PhysRevB.81.224510 PACS number(s): 74.45.+c, 74.50.+r, 74.78.Fk

The Andreev reflection (AR) was proposed in 1964 at a normal-metal/superconductor (N/S) interface,[1] and applied by Blonder, Tinkham, and Klapwijk (BTK) (Ref. 2) to N/S microconstriction contacts to describe the crossover from metallic to tunnel junction behavior. In recent years, the AR idea has been widely applied to study the ferromagnet/superconductor (F/S) junctions, multiterminal N/S or F/S structures, and graphene-based N/S or F/S junction, a number of new physical effects emerging. There is a virtual AR process at the F/S junction[3–6] in which the AR may become evanescent wave depending on the injection angle of the quasiparticle due to the Fermi-surface mismatch between spin-up and spin-down components, making the AR-induced current largely suppressed. In the multiterminal structures, there is a crossed AR (Refs. 7 and 8) in which the incident electron and the retroreflected hole may be transmitted through different contacts, as long as the distance between the two contacts does not exceed the superconducting coherent length. A graphene-based N/S or F/S junction may exhibit both Andreev retroreflection and specular AR due to the unique energy-band structures of graphene[9] and there is a transition between them with varying the exchange energy of the ferromagnetic graphene.[10]

In various AR mentioned above, the incident electron and the Andreev-reflected hole belong to different spin subbands, leading to a singlet pairing with opposite spins in the S. Here we propose a type of AR effect at the F/S interface with spin flip in which the incident electron and the Andreev-reflected hole belong to the same-spin subband, forming the singlet pairing via spin flip at the interface. For a half-metallic F (HMF)/S junction since in the HMF, there is only one spin channel for electrons at the Fermi level, the conventional AR cannot occur at the HMF/S interface but the same-spin-band AR can do. Recently, Keizer *et al.*[11] reported a long-range Josephson supercurrent between two *s*-wave superconducting NbTiN electrodes through a half-metallic CrO_2. Since singlet Cooper pairs cannot exist in the HMF, it was assumed[11–18] that a spin-triplet supercurrent passes through the HMF and a conversion from the spin-singlet to spin-triplet pairing takes place at the F/S interfaces. This result can be understood by the same-spin-band AR processes of quasiparticles with energy smaller than the superconducting energy gap. In the half-metallic region, a spin-up electron impinging on one of the interfaces is same-spin-band Andreev reflected and converted into a hole still in the spin-up subband moving in the opposite direction, thus generating a singlet Cooper pair in one S due to the spin-flip scattering at the interface. This hole in the spin-up subband is consequently same-spin-band Andreev reflected at the second interface and is converted back to a spin-up electron, leading to the destruction of the Cooper pair in the other S. As a result of this cycle, a singlet Cooper pair is transferred from one S to another, with the aid of a pair of correlated electron and hole in the same-spin subband of the half-metallic link, both of them being converted into each other via the same-spin-band AR at the two interfaces.

To make this theoretical explanation creditable, it is necessary to verify the existence of the same-spin-band AR effect by designing an experiment as simple as possible and by predicting a distinguishing mark. In this work, we extend the approach developed by BTK (Ref. 2) to study the conductance spectra in F/*s*-wave S contacts by taking into account interfacial potentials with spin flip. This potential at the F/S interface can be regarded as an effective interfacial potential of an F/F/S structure with noncollinear magnetization[19] in the limit of the thickness of the middle F layer tending vanishing. It is found that not only the conventional AR but also the same-spin-band AR may appear at F/S interfaces in the presence of spin-flip scattering. More interestingly, for the HMF/*s*-wave S contacts, only the same-spin-band AR occurs at the interface with spin flip. Its distinguishing mark is the zero-bias conductance vanishing (ZBCV) and finite V-shape conductance within the energy gap, which is called the ZBCV feature here. To be able to observe the ZBCV feature induced by the same-spin-band AR in experiments, three conditions are necessary: the F is half metallic, the S is *s*-wave pairing, and the spin flip is present at the F/S interface. If these conditions are satisfied, such a ZBCV feature will be obtained. With the spin polarization of the F deviated from 1, the ZBCV evolves a zero-bias conductance dip (ZBCD), the latter being also easily distinguished. As a result, the ZBCV (ZBCD) feature can be regarded as a distinguishing mark of the half-metallic (strongly spin-polarized) F. From a serious symmetric study, it is found that the ZBCV

feature obtained arises from the electron-hole symmetry at the Fermi level for the AR in the same-spin subband.

Consider an F/*s*-wave S junction in which the F and the S are separated by an interface at $x=0$. To capture the essential effect of the interfacial scattering with spin flip, we model it by a 4×4 matrix form

$$\hat{H}_I = \begin{pmatrix} U_1\hat{I}+U_2\hat{\sigma}_y & 0 \\ 0 & -U_1\hat{I}+U_2\hat{\sigma}_y \end{pmatrix}\delta(x) \tag{1}$$

with $\hat{\sigma}_y$ as the Pauli matrix and $\hat{I}$ the unit matrix acting in spin space. Here U_1 is the interfacial scattering potential in the BTK approach and U_2 plays a part of the spin flip at the interface. The Hamiltonian of the S is described by the BCS one of 4×4 matrix,

$$\hat{H}_{SC} = \begin{pmatrix} H_0\hat{I} & i\Delta\hat{\sigma}_y \\ -i\Delta\hat{\sigma}_y & -H_0\hat{I} \end{pmatrix}\Theta(x), \tag{2}$$

where $H_0=-\hbar^2\nabla^2/2m+V(x)-E_F$ is the free-electron Hamiltonian with $V(x)$ as the potential energy and E_F the Fermi energy, Δ is the superconducting pair potential, and $\Theta(x)$ is the unit step function. The Hamiltonian of the F is given by

$$\hat{H}_F = \begin{pmatrix} \left(H_0+\frac{h_0}{2}\right)\hat{I}-\frac{h_0}{2}\hat{\sigma}_z & 0 \\ 0 & -\left(H_0+\frac{h_0}{2}\right)\hat{I}+\frac{h_0}{2}\hat{\sigma}_z \end{pmatrix}\Theta(-x) \tag{3}$$

with h_0 as the exchange energy. For simplicity, it has been assumed here that the spin-up subband of the F and the band of the S have the same energy bottom, which dose not change the main results of this work. If we define $h_0=ME_F$, the condition of the HMF is $M\geq1$, for which the whole spin-down subband is above E_F so that the Fermi level cuts across only the spin-up subband.

By use of the Bogoliubov-de Gennes (BdG) equation, the BTK approach[2] is extended to study the F/S junctions. This approach has been widely applied to describing quasiparticle states in the S with spatially varying pair potentials. In the present F/S junction with spin flip, the quasiparticle states must be expressed by four-spinor wave functions. In the ferromagnetic region, the basis wave functions are given by $\hat{e}_1=(1,0,0,0)^T$, $\hat{e}_2=(0,1,0,0)^T$, $\hat{e}_3=(0,0,1,0)^T$, and $\hat{e}_4=(0,0,0,1)^T$, respectively, for the spin-up electron, spin-down electron, spin-up hole, and spin-down hole. Consider a spin-up electron with energy E just above E_F incident on the interface at $x=0$ from the left F. With general solutions of the BdG equation, the wave function for $x<0$ is given by

$$\Psi_L(x) = (e^{ik_{e\uparrow}x}+b_1e^{-ik_{e\uparrow}x})\hat{e}_1 + b_2e^{\kappa_{e\downarrow}x}\hat{e}_2 + a_2e^{ik_{h\uparrow}x}\hat{e}_3 + a_1e^{\kappa_{h\downarrow}x}\hat{e}_4, \tag{4}$$

where $k_{e(h)\uparrow}\approx k_F$ and $\kappa_{e(h)\downarrow}\approx\sqrt{M-1}k_F$ for $M\geq1$ and $\mp i\sqrt{1-M}k_F$ for $M<1$, with k_F as the Fermi wave vector. Here coefficients b_1, b_2, a_2, and a_1 correspond, respectively, to the normal reflection, the normal reflection with spin flip, the AR in the spin-up subband, and the conventional AR in the spin-down subband. In the case of the HMF ($M\geq1$), both the normal reflected electron and the Andreev-reflected hole in the spin-down subband are evanescent waves. In the right S region of $x>0$, we have

$$\psi_R(x) = c_1\hat{e}_5e^{ik_+x}+c_2\hat{e}_6e^{ik_+x}+d_2\hat{e}_7e^{-ik_-x}+d_1\hat{e}_8e^{-ik_-x}. \tag{5}$$

Here $\hat{e}_5=(u,0,0,v)^T$, $\hat{e}_6=(0,u,-v,0)^T$, $\hat{e}_7=(0,v,-u,0)^T$, and $\hat{e}_8=(v,0,0,u)^T$ are the basis wave functions, respectively, for the spin-up and spin-down electronlike quasiparticles (ELQs), and the spin-up and spin-down holelike quasiparticles (HLQs), which are obtained from $\hat{H}_{SC}\psi=E\psi$ with E measured from E_F. In Eq. (5), $k^{\pm}\approx k_F$, $u=\sqrt{(E+\Omega)/2W}$, and $v=\sqrt{(E-\Omega)/2W}$, with $\Omega=\sqrt{E^2-\Delta^2}$ and $W=E$ for $E\geq\Delta$, and $\Omega=i\sqrt{\Delta^2-E^2}$ and $W=\Delta$ for $E<\Delta$. If the spin-flip scattering is absent, the four-component BdG equation may be decoupled into two sets of two-component equations: one for the spin-up ELQ and spin-down HLQ wave functions $\hat{e}_5$ and $\hat{e}_8$, the other for $\hat{e}_6$ and $\hat{e}_7$.

The coefficients in Eqs. (4) and (5) can be determined by matching boundary conditions at the interfaces, yielding

$$\Psi_L(0_-)=\Psi_R(0_+),$$

$$\frac{\partial}{\partial x}\Psi_R(0_+)-\frac{\partial}{\partial x}\Psi_L(0_-) = 2k_F\begin{pmatrix} Z_1\hat{I}+Z_2\hat{\sigma}_y & 0 \\ 0 & Z_1\hat{I}-Z_2\hat{\sigma}_y \end{pmatrix}\Psi_L(0_-), \tag{6}$$

where $Z_2=U_2/\hbar v_F$ and $Z_1=U_1/\hbar v_F$ are dimensionless parameters describing the interfacial scattering with and without spin flip, respectively, with v_F as the Fermi velocity.

The zero-temperature differential conductance of the present tunnel junction can be obtained as $\sigma(E)=\sigma_\uparrow(E)+\sigma_\downarrow(E)$, where

$$\sigma_\uparrow(E)=\frac{e^2}{h}(1+M)[1+|a_2|^2-|b_1|^2+(|a_1|^2-|b_2|^2)\sqrt{1-M}], \tag{7}$$

for $M<1$, and $\sigma_\downarrow(E)$ is given in a similar way with a spin-down electron ($\hat{e}_2$) impinging on the barrier. In the case of the HMF ($M\geq1$), there are no spin-down incident electrons, and the normal reflected electron and the Andreev-reflected hole in the spin-down subband have no contribution to the conductance, so that $\sigma(E)=(2e^2/h)(1+|a_2|^2-|b_1|^2)$. For energies below the gap ($|E|<\Delta$), the current conservation reads $|b_1|^2+|a_2|^2=1$ and the differential conductance reduces to $\sigma(E)=(4e^2/h)|a_2|^2$. It indicates that in the HMF case, the conductance spectrum within the gap arises only from the same-spin-band AR.

It is well known that, for an HMF/*s*-wave S junction, the conductance within the energy gap should be zero in the absence of spin-flip effect at the interface, as shown by the solid line in Fig. 1. This is because the conductance within the gap arises from the conventional AR in the spin-down subband but there is no spin-down electron band across E_F in a half metal. Figure 1 shows the conductance spectra for different Z_2 with $M=1$ and $Z_1=0$. The presence of Z_2 leads

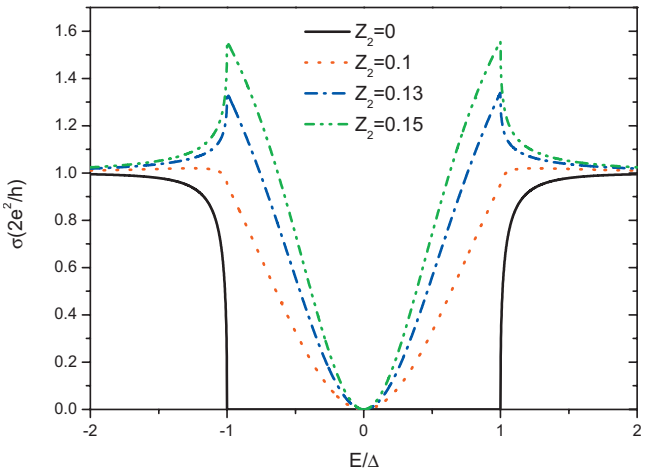

FIG. 1. (Color) Differential conductance spectra of HMF/s-wave S junctions for $M=1$ and $Z_1=0$ with various Z_2 indicated.

to conductance structures within the gap, which must arise from the AR in the spin-up subband. A most conspicuous sign there is the ZBCV feature, the conductance vanishing at $E=0$ and finite V-shape conductance within the energy gap. The present $Z_1=0$ corresponds to the metallic contact in the BTK theory, and nonzero Z_2 plays a part in the spin-flip scattering at the interface. With increasing Z_2, the V-shape conductance within the gap is enhanced by the increasing spin-flip scattering, as shown in Fig. 1. If Z_1 is increased with Z_2 fixed, the V-shape conductance within the gap will gradually decrease due to the suppression of the same-spin-band AR effect, and finally evolve into the U-shape one in the tunnel junction.

The ZBCV and finite V-shape conductance shown in Fig. 1 can be interpreted only by the same-spin-band AR, rather than by the conventional AR. This is because (i) the finite-conductance structure arises from the AR, (ii) the conventional AR needs two spin subbands on the metallic side, and (iii) the half metal has only one spin subband across the Fermi level. The present conclusion is a general one, depending neither on the BTK approach nor on the choice of parameters used here. As a result, the ZBCV feature can be regarded as a distinguishing mark of the same-spin-band AR appearing at an HMF/s-wave S interface.

What is the origin of the conductance vanishing at $E=0$? It comes from the electron-hole symmetry in the same-spin subband, which is unique in the same-spin-band AR process. Define an electron-hole transformation $U=\check{\tau}_x\otimes\hat{I}$, where $\check{\tau}_x$ is the Pauli matrix acting in the electron-hole space and $\hat{I}$ is the unit matrix in the spin space. After this transformation, the spin-up and spin-down electrons $\hat{e}_1$ and $\hat{e}_2$ become the holes $\hat{e}_3$ and $\hat{e}_4$ in the spin-up and spin-down band, respectively. For the s-wave paring, the pair potential is antisymmetric by interchanging the spin indices ($\Delta_{\uparrow\downarrow}=-\Delta_{\downarrow\uparrow}$) so that both the single-particle term and the pairing term in Eq. (2) change the sign under the U transformation. Therefore, for the Hamiltonian in the F, in the s-wave pairing S, or at the interface, we all have $U\hat{H}U^{-1}=-\hat{H}^*$, which leads to an electron-hole symmetry lying at the Fermi level ($E=0$).

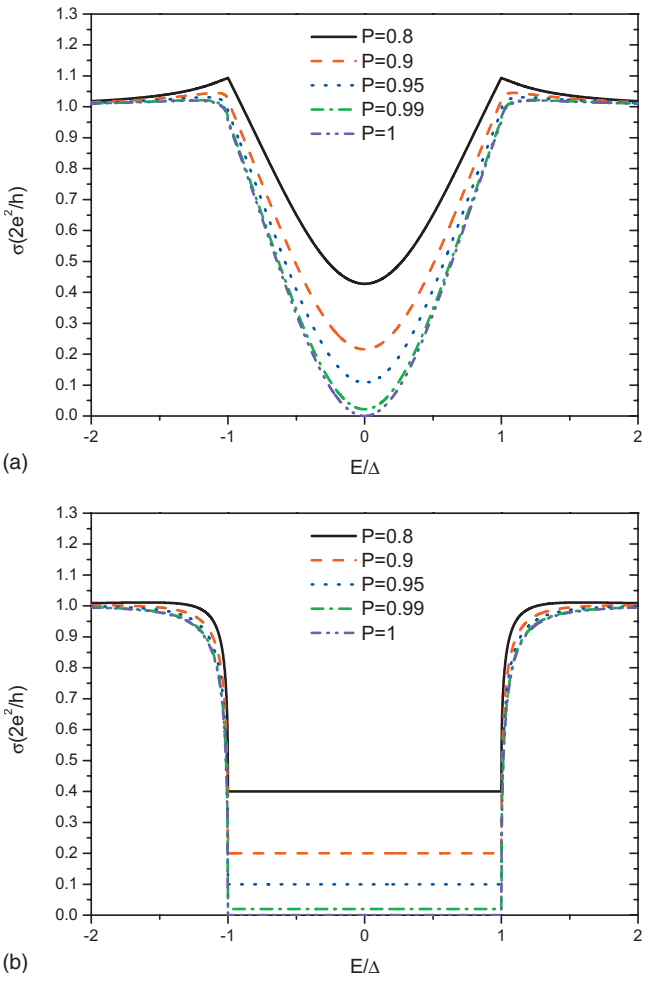

FIG. 2. (Color) Differential conductance spectra of strongly polarized F/s-wave S contacts ($Z_1=0$) for (a) $Z_2=0.1$ and (b) $Z_2=0$ with various P indicated.

In the HMF case, only the spin-up band crosses the Fermi level and contributes to the conductance. Consider the scattering processes of the electrons and holes in the spin-up band incident on the interface and reflected as electrons and holes in the same-spin subband of the left HMF. The incident wave function is $(e_{\text{in}},h_{\text{in}})^T$ and the reflected one is given by

$$\begin{pmatrix} e_{\text{out}} \\ h_{\text{out}} \end{pmatrix} = S\begin{pmatrix} e_{\text{in}} \\ h_{\text{in}} \end{pmatrix} = \begin{pmatrix} b_1 & a_2' \\ a_2 & b_1' \end{pmatrix}\begin{pmatrix} e_{\text{in}} \\ h_{\text{in}} \end{pmatrix}, \tag{8}$$

where coefficients a_2 and b_1 indicate the same-spin-band AR and the normal reflection processes for an incident electron, respectively, and a_2' and b_1' indicate the corresponding processes for an incident hole. In the HMF, only one spin subband is involved in the scattering and the matrix U is reduced to $\check{\tau}_x$ acting only in the electron-hole space. At the Fermi level, the electron-hole symmetry requires that $\check{\tau}_x S\check{\tau}_x^{-1}=S^*$, which leads to $a_2'=a_2^*$ and $b_1'=b_1^*$. The conservation of the particle numbers requires the unitarity of the S matrix and finally we get $a_2^*b_1=0$. Since the choice of $b_1=0$ and $|a_2|=1$ is impossible in the presence of tunnel barrier ($Z_2\neq 0$), the sole choice is $a_2=0$ at $E=0$, resulting in the ZBCV. The argument above indicates that the electron-hole symmetry at

$E=0$ for the same-spin-band AR is responsible for the ZBCV found in the present work. For $E\neq 0$, the electron-hole symmetry is broken and a finite conductance comes into being. For an N/S contact in the conventional BTK approach, since the incident electron and the Andreev-reflected hole are in two different spin subbands, the transformation U cannot be reduced to a 2×2 matrix $\check{\tau}_x$ acting only in the electron-hole space but maps $\hat{e}_5$ and $\hat{e}_8$ in one current channel into $\hat{e}_6$ and $\hat{e}_7$ in another channel. In this case, it can be easily shown that the zero-bias conductance is finite in metallic limit. We also wish to point out that the electron-hole symmetry above for the *s*-wave S may not be valid for the anisotropic S in which the ELQ and HLQ moving along the same direction feel the pair potentials with opposite signs,[20] which may result in the absence of the ZBCV. Therefore, the ZBCV feature here is a hallmark of the HMF/*s*-wave S contact with the distinct AR and spin-flip effect at the interface, protected by the electron-hole symmetry in the same-spin subband.

For the ZBCV feature as a result of the same-spin-band AR alone, its appearance requires that the F is half metallic. For an F of $P<1$ with P as the spin polarization, since the conventional AR also has contribution to $\sigma(E)$, the ZBCV evolves a ZBCD, as shown in Fig. 2(a). With P deviated from 1, the ZBCD is suppressed gradually and even disappears for small P. As a result, using an F/*s*-wave S contact with spin-flip scattering at the interface, one can distinguish the half metal from the ferromagnetic metal of $P<1$ by the ZBCV or ZBCD feature. The closer to the ZBCV the ZBCD is, the closer to 1 the spin polarization is. As a result, the ZBCD feature can be regarded as a mark of a strong spin polarization of the F. If the spin flip is absent ($Z_2=0$), each V-shape conductance curve with ZBCD becomes a horizontal line of $2(1-P)$ within the gap, as shown in Fig. 2(b). In this case, there is no same-spin-band AR so that the conventional AR alone is responsible for the conductance spectra.

Finally we wish to make a comparison between the present theory and related experiments. It was reported[11] that CrO_2 is a half metal with $P\simeq 0.96$ close to 1. Experimental conductance vs bias voltage for Nb/CrO_2 point contacts ($Z=0$) measured at 1.8 K showed a V-shape curve within the energy gap, whose zero-bias conductance is close to vanishing.[21] The similar V-shape conductance was also observed in Pb/CrO_2 point contacts, as shown by Fig. 4b of Ref. 22. Such a finite V-shape conductance is in qualitative agreement with curves in Figs. 1 and 2(a) but does not agree with the sharp U-shape one shown in Fig. 2(b). It then follows that the present theory can reproduce essential features of conductance spectra in the HMF/*s*-wave S contacts, and provide a more reasonable physical explanation for experimental results. Nadgorny *et al.*[23] used the point-contact AR technique to carry out a systematic study of the spin polarization in $La_{0.7}Sr_{0.3}MnO_3$ and applied a modified BTK model with two adjustable parameters: P and Z, to well fit the experimental data for $P\simeq 0.6$. In our opinion, however, such a fitting will be more and more difficult with P further increasing toward 1. In contrast, the same-spin-band AR provides a natural physical mechanism for the finite-conductance structure within the energy gap even at $P=1$. From Fig. 2(a), it follows that the present theory is suitable not only to $P=1$ but also to the case of $P<1$.

In summary, we have extended the BTK approach to study the HMF/*s*-wave S contacts and to find the ZBCV feature in their conductance spectra, which is protected by the electron-hole symmetry in the same-spin subband. The experimental observation of the ZBCV feature will provide a conclusive proof for the same-spin-band AR. The ZBCV or ZBCD feature can also be a distinguishing mark for the half-metallic or strongly polarized F.

This work is supported by the State Key Program for Basic Research of China under Grants No. 2006CB921803, No. 2009CB929504, and No. 2010CB923401.

[1] A. F. Andreev, Sov. Phys. JETP **19**, 1228 (1964).
[2] G. E. Blonder, M. Tinkham, and T. M. Klapwijk, Phys. Rev. B **25**, 4515 (1982).
[3] J. X. Zhu, B. Friedman, and C. S. Ting, Phys. Rev. B **59**, 9558 (1999).
[4] S. Kashiwaya, Y. Tanaka, N. Yoshida, and M. R. Beasley, Phys. Rev. B **60**, 3572 (1999).
[5] I. Žutić and O. T. Valls, Phys. Rev. B **61**, 1555 (2000).
[6] Z. C. Dong, D. Y. Xing, Z. D. Wang, Z. Zheng, and J. Dong, Phys. Rev. B **63**, 144520 (2001).
[7] J. M. Byers and M. E. Flatte, Phys. Rev. Lett. **74**, 306 (1995).
[8] G. Deutscher and D. Feinberg, Appl. Phys. Lett. **76**, 487 (2000).
[9] C. W. J. Beenakker, Phys. Rev. Lett. **97**, 067007 (2006).
[10] Q. Zhang, D. Fu, B. Wang, R. Zhang, and D. Y. Xing, Phys. Rev. Lett. **101**, 047005 (2008).
[11] R. S. Keizer, S. T. B. Goennenwein, T. M. Klapwijk, G. Miao, G. Xiao, and A. Gupta, Nature (London) **439**, 825 (2006).
[12] M. Eschrig, J. Kopu, J. C. Cuevas, and G. Schön, Phys. Rev. Lett. **90**, 137003 (2003).
[13] M. Eschrig, T. Löfwander, T. Champel, J. C. Cuevas, J. Kopu, and G. Schön, J. Low Temp. Phys. **147**, 457 (2007).
[14] M. Houzet and A. I. Buzdin, Phys. Rev. B **76**, 060504(R) (2007).
[15] M. Eschrig and T. Lofwander, Nat. Phys. **4**, 138 (2008).
[16] R. Grein, M. Eschrig, G. Metalidis, and G. Schön, Phys. Rev. Lett. **102**, 227005 (2009).
[17] V. Braude and Yu. V. Nazarov, Phys. Rev. Lett. **98**, 077003 (2007).
[18] Y. Asano, Y. Tanaka, and A. A. Golubov, Phys. Rev. Lett. **98**, 107002 (2007).
[19] Z. Ping Niu and D. Y. Xing, Phys. Rev. Lett. **98**, 057005 (2007).
[20] S. Kashiwaya and Y. Tanaka, Rep. Prog. Phys. **63**, 1641 (2000).
[21] R. J. Soulen, M. S. Osofsky, B. Nadgorny, T. Ambrose, P. Broussard, S. F. Cheng, J. Byers, C. T. Tanaka, J. Nowack, J. S. Moodera, G. Laprade, A. Barry, and M. D. Coey, J. Appl. Phys. **85**, 4589 (1999).
[22] Y. Ji, G. J. Strijkers, F. Y. Yang, and C. L. Chien, Phys. Rev. B **64**, 224425 (2001).
[23] B. Nadgorny *et al.*, Phys. Rev. B **63**, 184433 (2001).